

**Multicomponent measurement of respirable quartz, kaolinite and coal dust using fourier transform infrared spectroscopy (FTIR): a comparison between partial least squares and principal component regressions**

STACEY, Peter <<http://orcid.org/0000-0002-2689-2890>>, CLEGG, Francis <<http://orcid.org/0000-0002-9566-5739>> and SAMMON, Chris <<http://orcid.org/0000-0003-1714-1726>>

Available from Sheffield Hallam University Research Archive (SHURA) at:

<http://shura.shu.ac.uk/30152/>

---

This document is the author deposited version. You are advised to consult the publisher's version if you wish to cite from it.

**Published version**

STACEY, Peter, CLEGG, Francis and SAMMON, Chris (2021). Multicomponent measurement of respirable quartz, kaolinite and coal dust using fourier transform infrared spectroscopy (FTIR): a comparison between partial least squares and principal component regressions. *Annals of Work Exposures and Health*.

---

**Copyright and re-use policy**

See <http://shura.shu.ac.uk/information.html>

Multicomponent measurement of respirable quartz, kaolinite and coal dust using Fourier Transform Infrared spectroscopy (FTIR): A comparison between partial least squares and principal component regressions.

Peter Stacey<sup>\*\*\*</sup>, Francis Clegg<sup>\*\*</sup>, and Christopher Sammon<sup>\*\*</sup>.

\*Health and Safety Executive, Harpur Hill, Buxton, Derbyshire, SK17 9JN, United Kingdom

\*\*Sheffield Hallam University, Materials and Engineering Research Institute, Sheffield, S1 1WB United Kingdom

## Supplementary Information

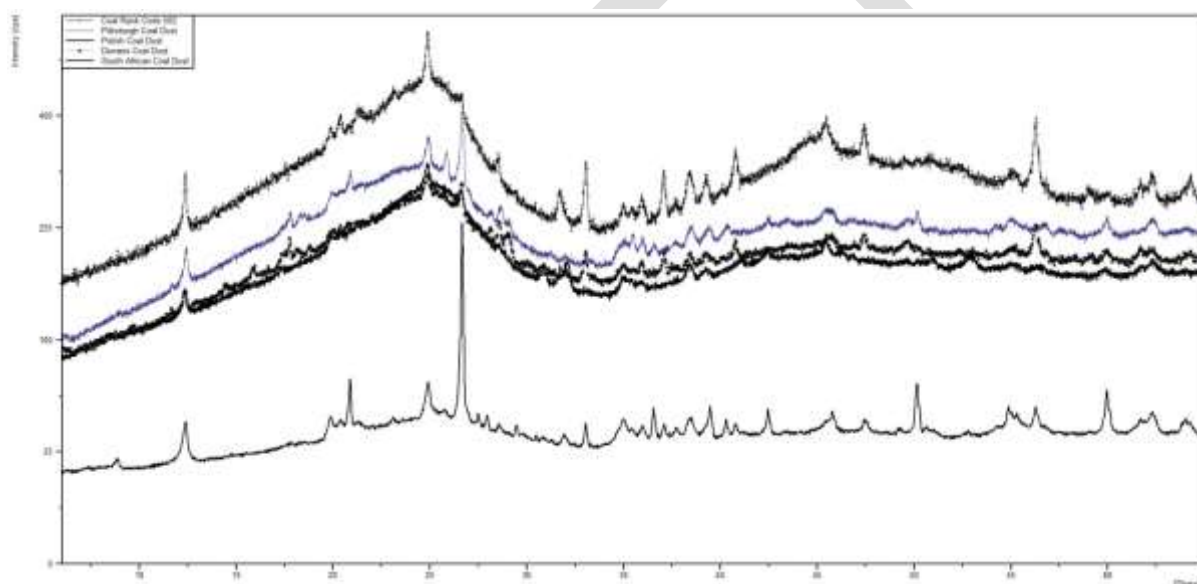


Figure S1. X-ray diffraction scans from a selection of powdered coals.

X-ray diffraction analysis for the determination of the assigned target values.

### Measurement conditions

For quartz, the instrument used the second set of standard instrumental conditions described in Table A1 of the International Standards Organization (ISO) standard method ISO 16258-1; 2015 (ISO, 2015). The instrument was fitted with a broad focus copper tube set at 50 kW and 45 mA, automatic scattering and receiving slits set to provide an illumination length of 18 mm, and an array detector with the detection area set at a  $2\theta$  range of 2.12 degrees. The area of the three most intense XRD reflections of quartz at  $2\theta$  angles of, 20.9, 26.6 and 50.1 degrees were measured for 600 seconds, 420 s and 600 s, respectively, for each 0.03  $2\theta$  degree interval over the two degree range centered

on the measurement reflection. The total sample analysis time was about 30 minutes. Tube drift was corrected using the measurement of an aluminium plate as an external standard. The average of the two most consistent results obtained from the three reflections was used as the quartz 'assigned' target value when significant interference was present that affected one of the XRD reflections. Generally, the reflection at  $20.9\ 2\theta$

For kaolinite, the area of the two most intense reflections free from quartz interference at  $2\theta$  positions of  $12.2$  and  $25$  degrees were used for quantification. A scan of a sample was collected from  $6$  to  $60$  degrees in steps of  $0.02$  and  $60$  s per step. The total scan time was 25 minutes. Each measurement reflection was quantified using a  $2\theta$  range of two degrees. The average of the two results obtained from each of the kaolinite measurement reflections was used as the kaolinite 'independent' value.

X-ray diffraction calibration charts are shown in Figures S2 and S3 overleaf.

DRAFT

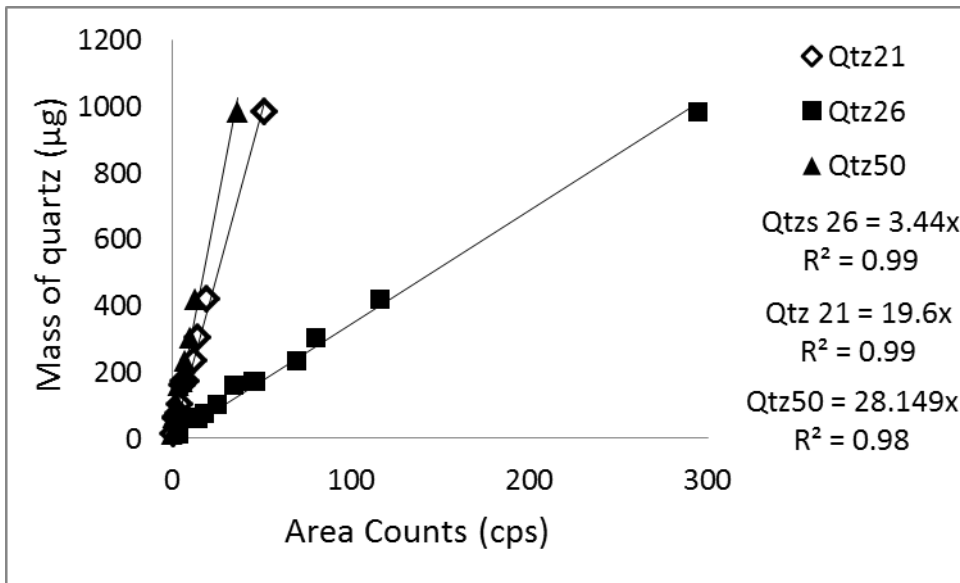


Figure S2. Trend line for the relationship between mass of quartz standard A9950 collected on a filter using the SIMPEDS respirable sampler and X-ray diffraction area response for the principal quartz reflections at 2θ degrees of 20.9 (Qtz21), 26.6 (Qtz26) and 50.1 (Qtz50).

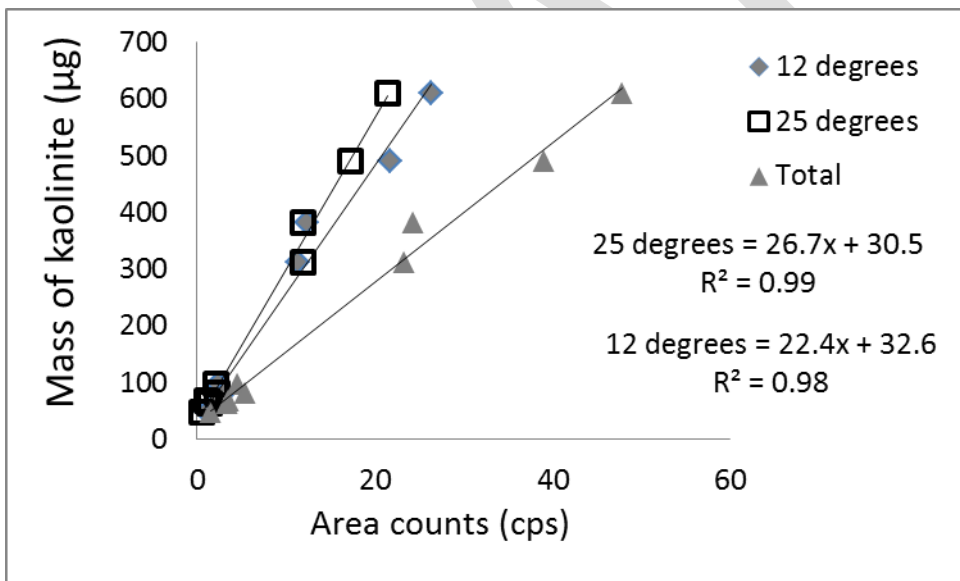


Figure S3. Trend line for the relationship between mass of kaolinite standard (Georgia, USA) collected on a filter using the SIMPEDS respirable sampler and X-ray diffraction area response for the principal kaolinite reflections at 2θ positions of 12 and 25 degrees.

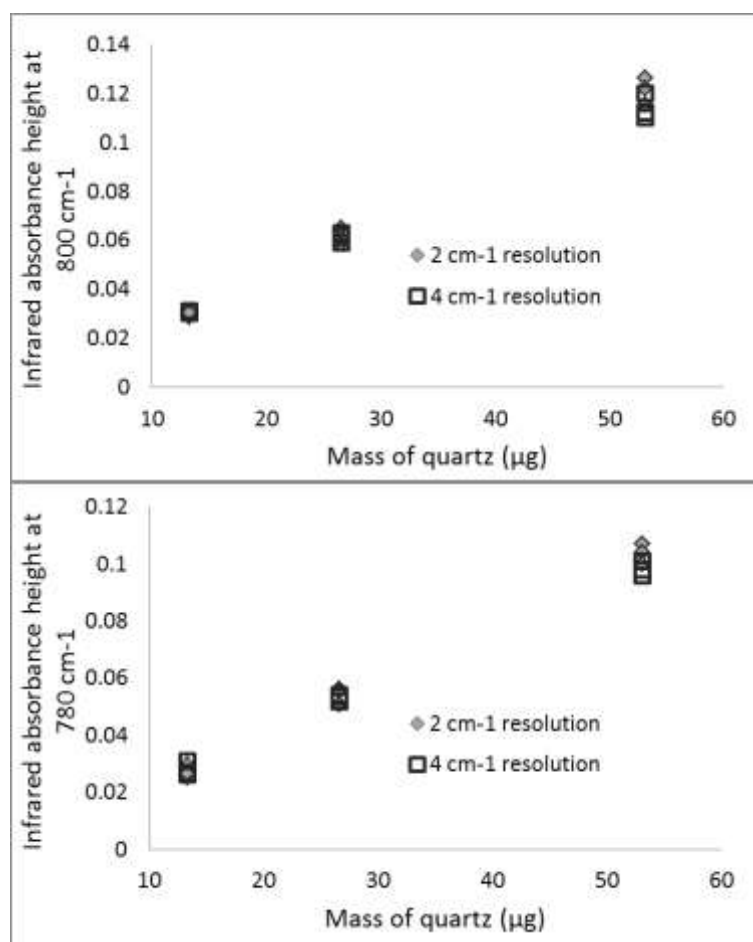


Figure S4. Infrared absorbance at 800  $\text{cm}^{-1}$  and 780  $\text{cm}^{-1}$ , when measuring three replicate aliquots quartz at three different mass loadings deposited onto polyvinylchloride filters at two different spectral resolutions of 4  $\text{cm}^{-1}$  and 2  $\text{cm}^{-1}$ .

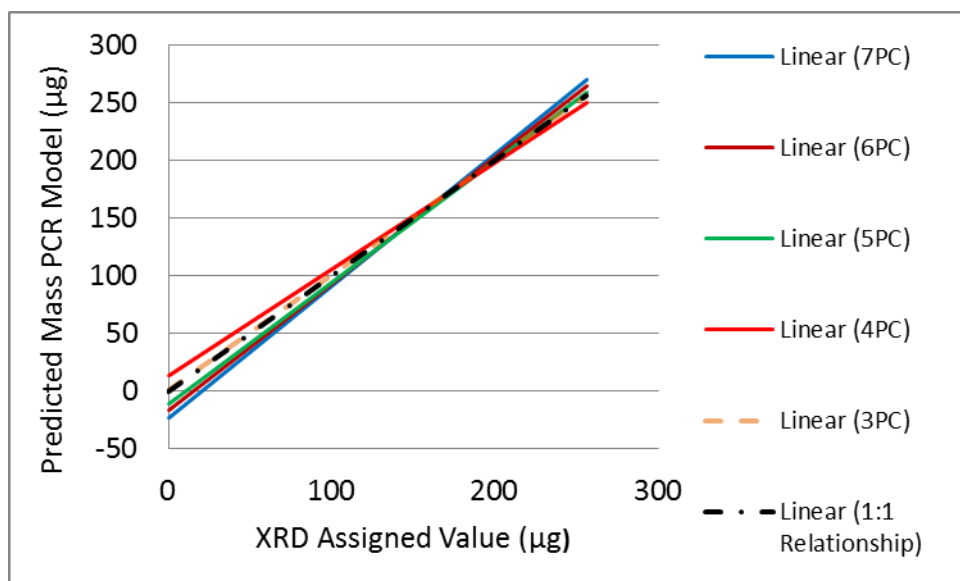


Figure S5. Change in the slope of the relationship between the predicted mass and the XRD assigned value for quartz as the number of principal components are changed from 3 to 7.

Table S1. Regression coefficients and average difference for the principal component regression model shown in Figure S5 with 3 to 7 principal components (PC).

PC	Slope coefficient	Intercept coefficient ( $\mu\text{g}$ )	Average absolute difference ( $\mu\text{g}$ )
7	1.14	-23.0	17.2
6	1.09	-16.3	12.5
5	1.05	-10.7	9.4
4	0.927	13.2	12.1
3	0.996	1.16	5.6

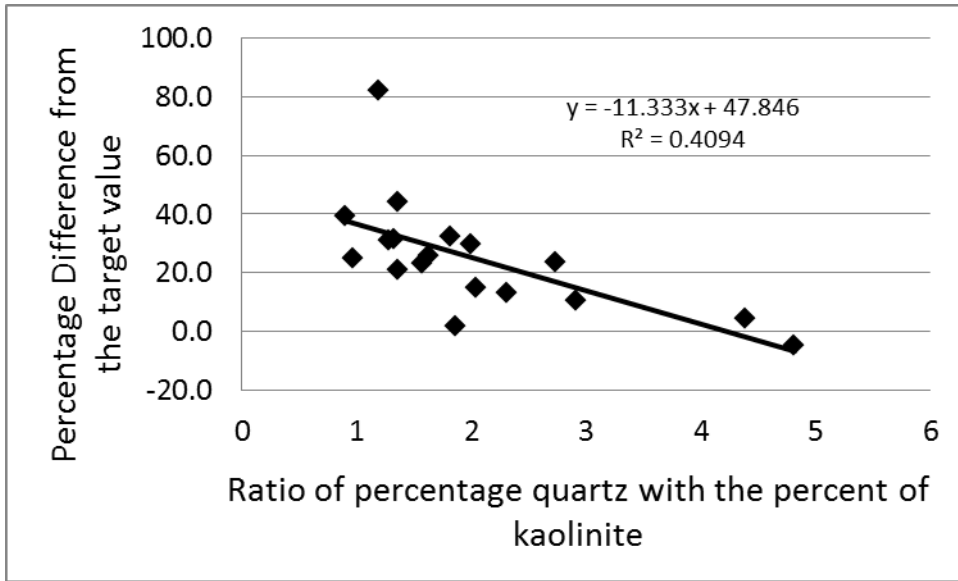


Figure S6. Chart showing the relationship between the proportion of kaolinite in the sample and its effect in on the magnitude of the error for the reported value when using infrared with MDHS 101.

DRAFT

Table S2. Composition and total gravimetric mass of samples used for the calibration set

Total Gravimetric Mass ( $\mu\text{g}$ )	Percent proportion of constituent mineral		
	Quartz	Kaolinite	Coal Dust
314.3	0.7	11.0	88.3
698.0	20.8	4.7	74.4
204.7	27.1	14.9	58.0
420.3	26.2	20.4	53.4
247.2	24.9	27.7	47.3
665.0	28.9	17.8	53.3
731.7	30.4	22.8	46.8
879.0	37.4	27.5	35.1
423.0	41.2	26.1	32.7
428.7	20.7	7.1	72.2
844.3	21.1	4.4	74.5
487.7	18.1	18.6	63.3
882.3	18.1	15.2	66.7
584.7	26.7	19.6	53.7
901.3	37.4	18.7	44.0
845.7	27.8	17.4	54.8
679.3	39.1	19.2	41.7
1010.7	42.2	18.2	39.6
1348.3	32.0	11.7	56.3
419.9	100		
302.5	100		
160.7	100		
99.9	100		
170.7	100		
234.5	100		
75.0	100		
171.8	100		
10.9	100		
60.6	100		
985.2	100		
62.9	100		
327.1		100	
107.1		100	
88.7		100	
99.7		100	
53.3		100	
88.9		100	
72.3		100	



60.9		100	
403.2		100	
478.3		100	
218.1		100	
55.4		100	
611.1		100	
489.5		100	
311.3		100	
382.4		100	
97.5		100	
67.2		100	
48.2		100	
81.5		100	
62.7		100	
518.4	89.6	10.4	
214.7	77.2	22.8	
120.9	64.2	35.8	
169.1	67.4	32.6	
183.6	49.9	50.1	
85.9	37.1	62.9	
202.0	39.8	60.2	
107.6	31.7	68.3	
222.4	26.3	73.7	
121.4	21.9	78.1	

Table S3. Total gravimetric mass of proportion of constituents in the samples used for the validation set

Total Gravimetric Mass ( $\mu\text{g}$ )	Percent proportion of constituent mineral		
	Quartz	Kaolinite	Coal Dust
100	100.0		
75	100.0		
74	18.3		81.7
142	28.0		72.0
98	19.2	46.0	34.7
192	17.6	44.7	37.7
143	26.3	37.8	36.0
339	26.1	60.9	12.9
277	38.9	32.3	28.7
169	37.1	27.4	35.4
238	42.1	31.0	26.9
176	19.3	39.6	41.1
181	34.2	37.9	27.9

362	27.8	25.8	46.3
205	32.8	46.8	20.4
1205	16.4	40.1	43.5
851	20.7	44.8	34.5
534	21.3	42.6	40.0
1255	20.4	40.4	39.2

Table S4. Total gravimetric mass of proportion of constituents in the samples used for the prediction set

Total Gravimetric Mass ( $\mu\text{g}$ )	Percent proportion of constituent mineral		
	Quartz	Kaolinite	Coal Dust
939.6		4.8	95.2
801.7		4.9	95.1
417.1	24.0		76.0
397.8	30.6		69.4
532.5	21.8	22.3	55.8
308.7	17.2	45.7	37.2
437.2	15.3	41.8	42.9
536.3	17.3	42.3	40.3
123.1		32.0	68.0
152.1	6.1		93.9
204.6	3.8	19.9	76.3
222.0	4.1	21.2	74.8
250.5	3.8		96.2
150.5	5.7		94.3
270.2	26.6	54.4	19.0
380.7	18.8	39.9	41.2
403.1	20.5	48.6	30.9
851.0	20.7	44.8	34.5
427.0	20.4	42.4	37.2
493.4	18.6	44.0	37.4
578.3	13.9	37.2	48.9
853.8	16.4	45.2	38.4
1204.8	16.4	40.1	43.5
1254.5	20.4	40.3	39.3
74.0	100.0		
99.9	100.0		
101.0	100.0	Proficiency testing samples	
135.0	100.0		
99.9	100.0		
74.0	100.0		
92.6	100.0		

86.7	100.0	
155.2	100.0	
196.6	100.0	

#### Comparison of background correction methods

Table S4 compares the results obtained when using the blank filter subtraction process outlined in MDHS 101 and with a first derivative processing of the scan to normalise the spectral background from the filter. Beers law models were developed for each background correction process. Each model was developed using the same calibration filters. Results from eight independent samples containing quartz standard are listed below:

Table S5. A comparison of results from two background correction processes.

Sample	Mass recorded by each method		Absolute difference ( $\mu\text{g}$ )	Percentage Difference
	Blank filter subtraction	First derivative processing		
T3	413 $\mu\text{g}$	401 $\mu\text{g}$	-12	-2.9 %
T4	94.5 $\mu\text{g}$	89.0 $\mu\text{g}$	-5.5	-5.8 %
T5	75.6 $\mu\text{g}$	71.2 $\mu\text{g}$	-4.4	-5.8 %
T6	465 $\mu\text{g}$	453 $\mu\text{g}$	-12	-3.2 %
T10	112 $\mu\text{g}$	106 $\mu\text{g}$	-6.0	-5.3 %
T13	45.6 $\mu\text{g}$	42.5 $\mu\text{g}$	-3.1	-6.8 %
T14	91.8 $\mu\text{g}$	85.6 $\mu\text{g}$	-6.2	-6.7 %
T16	15.8 $\mu\text{g}$	11.6 $\mu\text{g}$	-4.2	-26 %